

Simulation of Tile Drain Flows in an Alluvial Clayey Soil Using HYDRUS 1D

Rifat Akı̇s

Department of Soil Science and Plant Nutrition, Mustafa Kemal University,
College of Agriculture, 31034 Antakya / Hatay, Turkey

Abstract: Storm water flooding and inundation events require managing surface runoff and drainage water in the Amik Plain, Turkey. The objectives of this study were to i) determine tiling flow effects on soil moisture distribution profile ii) simulate drain-tile flows in a clayey soil and iii) compare drain hydrographs with simulated model drainage fluxes in the soil profile. The sandy loam (SL) site showed 88 m³/ha tile drainage, while silty clay loam (SiCL) site showed 71 m³/ha tile flow during the 32-day measurement period. The main's outlet showed 264 m³/ha of drain discharge to the streams, corresponding to 0.87% of total runoff. Drainage hydrograph measurements showed different peak flow rates and durations for the SiCL (2.9 cm/d, 33-days) and SL (3.2 cm/d, 28-days). The groundwater accretion was more effective than surface runoff events to limit cropping system in the plain. Hydrus-1D simulations calculated water table elevations ranging from 41 to 44 cm during calibration and validation periods of 82 days. The occurrence of variably saturated conditions and tile discharges varied based on the site-specific field conditions such as soil texture and saturated hydraulic conductivity. Therefore, a flood control and protection measures can be planned based on drain discharges in the field.

Key words: Drainage rate • Runoff • Tile flow • Subsurface drainage • Hydrus • Soil moisture • Piezometer • Amik Plain

INTRODUCTION

Amik plain soils are characterized by their heavy clay alluviums and poorly drained conditions owing to the fact that they are prone to heavy rain falls and floods and they have low saturated hydraulic conductivity. As a result, surface and sub-surface drainage practices are necessary in the Plain's soils for agricultural practices. There existed a lake, called as the Lake Amik, until 1975, which was entirely drained through surface open drain ditches and canals to the Mediterranean Sea between 1962 and 1975. The lake floor area holds predominantly low saturated hydraulic conductivity values. However, poorly drained conditions in the plain have not been totally vanished, but have been reduced all over the plain till today mostly because of salt leaching. Siltation is the major problem to the open drain canals that become incapacitated to remove rainfall excess in the plain. When floods happen, it takes reasonably long time to drain out of the plain. This causes big operation problems in tillage and harvest

times. The longevity of floods and high groundwater levels delay seedbed preparation in agronomic time table. The region practices two cropping cycles in rotation, in which wheat and cotton or cotton and corn are rotated in a year. Surface and sub-surface drainage practices are very crucially needed as a prevention measure for crops from floods and anaerobic conditions for a better growth and high yield quality and quantity in the plain. In the Amik Plain, drainage practices also serve for salt leaching and removal purposes to reduce salt accumulation hazards in the rooting depth of the plain soils, which is a very critical and important benefit one can gain from these drainage practices. Tile drainage practices in the Plain are invasively spread both by governmental and private sectors in these days. In general, drainage priority is given to large hectares of orchards and olive garden type plantations on these tile drained lands. The purpose of soil tile drainage activities is to remove excess water from the soil surface and profile and more critically delay the peak flows of surface runoff in the Amik Plain as a flood

prevention measure. Therefore, the effects of soil and rainfall characteristics on moisture profile distribution and drain tile discharges versus time in a rainy period are needed to investigate for a comprehensive understanding of tile flow effects on crop quality and quantity in the Plain. In the rainy period of the plain, rainfall excess accumulates in the foot lands that have slope of 0-2% [1, 2] and groundwater table soaks to the soil surface. In order to gain in-depth understanding of soil drainage flows and rainfall relations, modeling may be a useful alternative tool versus tedious field measurements. Water flow in the soil profile is assumed to be only in vertical direction in this study. This assumption is also suggested by Phogat *et al.* [3] and 1D model simulations are useful for many applications.

Soil hydraulic properties and rainfall characteristics effects on tile flow hydrograph is a very critical data to develop a sound drainage system design in the plain. Ebrahimian *et al.* [4] showed that drain depth and space parameters could greatly influence drainage discharge-time relations in two soil types with cracks and macropores. In arid/semiarid ecosystems, drainage hydrograph can also be used for drainage water management purposes so that productive and unproductive soil water fluxes in the profile can be classed for effective water use in agriculture.

In arid climates, rainfall is limiting factor for ecosystem functions and, if any, shallow groundwater source is critically important for water needs. Therefore, surface water bodies and contributions to the surface water sources from the groundwater systems critically important for the ecosystem functions in arid and semiarid regions [5]. Ayers *et al.* [6] reported 50% of irrigation requirement of plants can be provided shallow groundwater sources available. In order to have a comprehensive understanding of the soil water potential, piezometric heads and drainage rates versus time relations, Hydrus-1D model was used to simulate tile water flow rates from the Amik Plain solis. The Hydrus model [7] was used to simulate water flow and chemical transport in furrow irrigation [4, 8], subsurface drainage discharge rates and pesticide concentrations [9], salt transport in irrigated rice paddy [3], prediction of root zone water and nitrogen balance in irrigated semi-arid regions of India [10].

The objectives of this study were to i) to determine tile flow effects on soil moisture distribution profile, ii) to evaluate drain tile response to piezometric heads because

of rainfall and iii) to simulate drain-tile flows for better drainage water management. In this study, Hydrus 1D simulation model and drainage hydrographs were evaluated. Simulation and observed results are compared and discussed in terms of drain depth and spacing, head gradients, drainage rates, drainage hydrographs.

MATERIALS AND METHODS

Site Details: The experiment was established on an alluvial clayey soil in 2010 in Tarla 49 research station of Mustafa Kemal University. The field elevation from the sea level was 71 m. The soil profile predominantly have a A horizon and an argillic B horizon (Bt). The climate of the region is semi-arid/semi-humid temperate. The mean annual rainfall is 1141 mm, approximately 70% of which occurs during rainy season (November-May). The mean annual evaporation is 1278 mm in the basin. The mean annual temperature over the last 50 years is 18.1°C.

Hydrus-1D Model

Water Retention Curves: Soil samples were collected to a depth of 100 cm for soil particle size analysis with Edelman auger and particle size analysis was performed by hydrometer method [11]. Undisturbed soil samples were collected by soil cores of 7.6 cm height x 7.6 cm diameter with 10 cm intervals in the soil profile. Soil saturated hydraulic conductivity (Ks) was measured for each depth according to [12] in two replica. Bulk density, porosity, water retention curves (WRC) and soil hydraulic parameters were determined on the undisturbed soil core samples in the laboratory. Starting from saturation water content, water discharges during successive matric potential decreases was measured on both tension table and porous pressure plate successively in at 0, -10, -15, -33 and -1500 kPa. The van Genuchten [13] and Mualem [14] equation was fitted to the data points.

Model Description: Water movement in soil profile and drain discharge rates from tiles in the soil profile were simulated using Hydrus-1D [7]. Vertical flow of water was simulated while using surface runoff and tile pipes as upper and lower boundary conditions in the flow domain. The Richards equation for saturated and unsaturated soil conditions was numerically solved in Hydrus-1D. The package also simulates soil solute and heat transport problems using the governing convection-dispersion equation in variably saturated porous media.

The Richards equation as follows:

$$\frac{\partial \theta}{\partial t} = \frac{\partial}{\partial z} \left[K(\theta) \left(\frac{\partial h}{\partial z} + 1 \right) \right] - S \quad (1)$$

where h is the water pressure head (cm), θ is the volumetric water content (cm^3/cm^3), t is the time (day), z is the measurement depth of soil (cm), $K(\theta)$ is unsaturated hydraulic conductivity function. Root water uptake is a sink in the Richards equation and therefore it is negatively signed in the equation.

The van Genuchten [13] model is given as the following.

$$\theta(h) = \begin{cases} \theta_r + \frac{\theta_s - \theta_r}{[1 + (\alpha|h_m|)^n]^m} & h \leq 0 \\ \theta_s & h \geq 0 \end{cases} \quad (2)$$

$$K(h) = K_s S_e^l \left[1 - \left(1 - S_e^{\frac{1}{m}} \right)^m \right]^2 \quad (3)$$

$$m = 1 - \frac{1}{n} \quad n > 1 \quad (4)$$

$$S_e = \frac{\theta - \theta_r}{\theta_s - \theta_r} \quad (5)$$

where, $\theta(h)$ is water retention curve function, θ_r the residual volumetric water content, θ_s saturated volumetric water content, h_m is the matric head (cm). The parameter α is air-entry parameter and m and n are retention curve fitting parameters. $K(h)$ is unsaturated hydraulic conductivity function computed from the water retention curve. K_s is saturated hydraulic conductivity. S_e is the reduced water content and l is the pore connectivity parameter with an estimated value of 0.5 [14].

The residual water content, θ_r , is the water content value below which water no longer be removed from the soil by plants and it is equal to wilting point water content of sandy soils. The hydraulic parameters of soil, θ_r , θ_s , θ_a and n , were initially determined from the measured soil water retention data according to van Genuchten [13] computational steps. Then, they were optimized using the RETC software by fitting retention data (θ - h relationship). These optimized values of hydraulic parameters were required in Hydrus-1D.

Initial and Boundary Conditions: Initial soil water content and pressure head for various soil layers within the flow domain were given as initial conditions for the water flow simulation model. The model assumed no water flow along

the boundaries (no flux boundary) of the research field. An atmospheric boundary condition with runoff was implemented along the top of the soil surface to allow for interactions between soil and atmosphere. These interactions contain rainfall, evapotranspiration and thus root water uptake in the time-variable boundary conditions. The bottom boundary was defined by several horizontal drain tiles. The drain tiles were assumed to have been installed in a homogeneous soil above impervious layer, whose discharges (fluxes) were calculated by steady-state conditions with Hooghoudt [15] equation in the Hydrus-1D.

Hooghoudt [15] equation as follows;

$$L^2 = \frac{4K_a h_t^2}{q} + \frac{8K_b d h_t}{q} \quad (6)$$

where, h_t is the water table level (m) at the midpoint between two laterals? K_a and K_b are the saturated hydraulic conductivity values (m.day^{-1}) above and below drain line, respectively. q is the drain discharge rate (m.day^{-1}), L is the drain spacing (m) between two laterals and d is the equivalent depth (m) of the drains.

Hydrus-1D uses Murrashima and Ogino [16] equation to modify soil saturated hydraulic conductivity to obtain a more appropriate value for K_s rather than the measured K_s in a thin layered soil as the following equation:

$$K = cK_s \quad (7)$$

where, c is conversion coefficient (dimensionless) and K_s is measured saturated hydraulic conductivity value (m.day^{-1}).

Drainage System and Meteorological Data Recordings:

A weather station was established in the field to record soil and air climate parameters on half hourly basis. Precipitation, evapotranspiration, leaf area index (LAI), soil matric potentials and soil temperatures were obtained from the meteorological weather station (VantagePro2, Davis Instrument, USA). Two automated moisture probes were installed in 0-30 cm and 30-90 cm depths in the profile. Drain tile flow was measured by automatic flow gauges connected to the lateral drains and the outlet of the main drainage pipe. Drain depth and spacing was 1 m and 37 m respectively. Four parallel laterals on one side of the main drain line were designed to discharge excess water from the study area to the main's outlet. A corrugated and perforated polyvinyl chloride (PVC) pipe

of 100 mm and 70 mm diameters for main collector and laterals were used in the drainage system design in the field. The impervious layer was assumed to be around 3 m depth in the soil profile. The field is prone to frequent surface and subsurface floods annually.

Atmospheric boundary conditions in the Hydrus-1D considers water evaporates at the potential rate in the soil surface as long as the pressure head at the soil surface is greater than a critical pressure head value, $h_{critical}$, the threshold value, -10000 cm in this study.

RESULTS AND DISCUSSION

Physical Properties of Soil Profiles for Buried Drain

Tiles: Lateral-1 is buried into the soil profile where clay content dominated over the sand and silt content in the depth range 0 to 50 cm. Lateral-3 was laid over a sandy loam, while lateral-1 was standing on a silty clay loam. Lateral-3 was draining a soil profile composed of eight loam and sandy loam layers at variant depths and silty clay loam layer in the surface soil. On the other hand, lateral 1 was draining a soil profile composed of two clay layers over a consequentially graded five clay loam layers over a base layer of silty clay loam at the 80 to 90 cm depth. In contrast to the lateral-1 and lateral-3 buried soil profiles, lateral-2 was buried in the soil profile with a textural turmoil (Table 1). As a result, the laterals 2 and 4 did not function appropriately to measure drainage discharges in a timely basis during the research period.

The hydraulic model parameters are presented in Table 2. Although water table and soil moisture content was measured continuously during the research period, the hydraulic model parameters were optimized only for the 30 to 90 cm depth. The top soil was very sensitive to precipitation and evapotranspiration, while the bottom layer was more consistent with its moisture potential distribution. Therefore, the hydraulic models simulated for the 30 to 90 cm depth.

Precipitation Evaporation and Transpiration in the Study

Site: Potential evaporation (E_p) and transpiration (T_p) were computed using Penman-Monteith [17] and Hydrus-1D Guide. The computation process uses reference crop ET_0 and leaf area index values. After E_p and T_p were calculated, their distributions during the study period against the precipitation in the study site are given in Fig. 1.

Pressure Head Measurements: Dynamics of water pressure head distribution in the soil profile is a result of precipitation frequency, evapotranspiration, soil water

content and groundwater table fluctuations. Soil pressure head values at the 0 to 30 cm depth and the 30 to 90 cm depth fluctuated because of water content differences of the soil profile (Fig. 2). In the first 7 days of the study, all soil profile desiccated (pressure heads between -500 and -2000 cm). On the day 8, groundwater reached at the soil depth of 90 cm, as a result of which pressure heads in the 30 to 90 cm layer steeply increased from -2000 to -500 cm. the effect of steep groundwater elevation in the 30 to 90 cm depth was seen on the pressure head fluctuations of the 0 to 30 cm depth (Fig. 2). The 0 to 30 cm depth registered more oscillatory behavior than the 30 to 90 cm depth pressure heads. In other words, the 0 to 30 cm layer responded to precipitation faster than the sub-layer 30-90 cm. There was, on average, a nine-day time interval between consecutive observed pressure head peaks in the studied period for 30 to 90 cm depth, while the time interval between the observed peaks of pressure heads of 0-30 cm layer was between 3 and 5 days (Fig. 2). In general, the 30-90 cm soil layer was always wetter than the 0-30 cm layer in the soil profile. Because of groundwater table fluctuations and natural precipitations, soil water pressure heads fluctuated at the 0 to 30 cm depth during the measurement period, while the pressure heads at the 30 to 90 cm depth showed very small changes, especially after the day 50 in the soil with limited evapotranspirations. These results are also reported by Li *et al.* [18] for water content.

Calibration and Validation of the Data

Pressure Head Distribution, Gradients and Simulations for the Lateral-1: Using soil hydraulic parameters estimated by RETC as the initial estimates, observed values of the pressure heads at soil depths of 0 to 30 cm and 30 to 90 cm during 82 days of rainy season in the Amik Plain were used for calibration and validation of the soil hydraulic parameters (θ_r , θ_s , α and n). Half of the pressure head values for 41 days were used in calibration period, while the rest of the data were used in the validation period of the hydraulic model for each soil profile depth of 90 cm. The correspondence of observed to simulated data for calibration period was moderately to fairly good for lateral-1 ($r^2=0.554$, $rmse = 0.217$), lateral-2 ($r^2 = 0.363$, $rmse = 0.215$) and for lateral-3 ($r^2 = 0.397$, $rmse = 0.579$), respectively. The calibrated parameters were used to simulate the rest of the data for the validation period and the statistics for drain laterals 1, 2 and 3 were 0.81, 0.353 and 0.657 for the r^2 values and 0.725, 0.579 and 0.643 for the $rmse$ values of validation period, respectively. The results are presented in Figure 3 for both calibration and validation period of the data.

Table 1: Soil textural classes and particle size distribution for each lateral

Sampling depth, cm	Clay, %	Sand, %	Silt, %	Textural Class	ρ_b , g.cm ⁻³
----- Lateral 1 -----					
0-10	46.9	6.7	46.4	SiCL	1.20
10-20	51.0	13.2	35.8	C	1.26
20-30	36.9	23.6	39.5	CL	1.42
30-40	42.6	25.2	32.2	C	1.32
40-50	35.6	27.1	37.3	CL	1.36
50-60	33.2	25.1	41.6	CL	1.22
60-70	31.3	28.2	40.5	CL	1.42
70-80	35.3	22.7	42.0	CL	1.37
80-90	38.8	18.6	42.6	SiCL	1.35
----- Lateral 2 -----					
0-10	42.5	20.4	37.1	C	1.14
10-20	34.1	33.3	32.6	CL	1.42
20-30	35.6	30.1	34.3	CL	1.36
30-40	41.9	17.7	40.4	C	1.16
40-50	39.3	19.4	41.3	SiCL/CL	1.13
50-60	40.1	24.1	35.9	CL/C	1.25
60-70	39.7	30.3	30.0	CL/C	1.37
70-80	43.6	20.8	35.6	C	1.15
80-90	23.8	50.4	25.7	SCL	1.44
----- Lateral 3 -----					
0-10	39.6	13.7	46.7	SiCL/SiC	1.31
10-20	24.7	36.7	38.6	L	1.39
20-30	19.9	43.7	36.3	L	1.43
30-40	19.4	49.5	31.1	L	1.5
40-50	12.5	67.0	20.6	SL	1.52
50-60	9.2	64.6	26.2	SL	1.55
60-70	14.6	51.7	33.7	SL/L	1.57
70-80	12.4	59.0	28.5	SL	1.61
80-90	10.2	62.9	26.9	SL	1.63

Table 2: Values of soil texture, bulk density (ρ_b), residual moisture content (θ_r), saturated water content (θ_s) and optimized van Genuchten soil hydraulic parameters (alpha (α) and n) used for the validation of the model

Laterals	θ_r	θ_s	α cm ⁻¹	n	Ks cm.d ⁻¹
----- Water table at 90 cm depth -----					
L1	0.0715	0.4583	0.0023	1.7374	10.2
L2	0.1	0.39	0.059	1.48	5.5
L3	0.0833	0.4701	0.0015	1.8561	6.56
L4	0.0733	0.4764	0.0039	1.5308	17.03

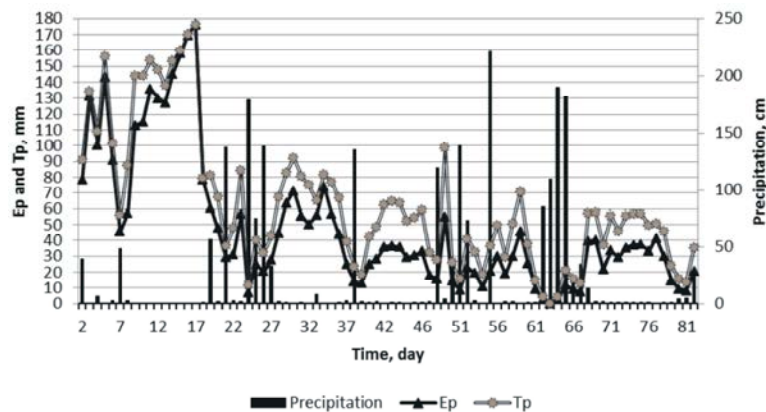


Fig. 1: Dynamics of potential evaporation, transpiration and precipitation in the study site

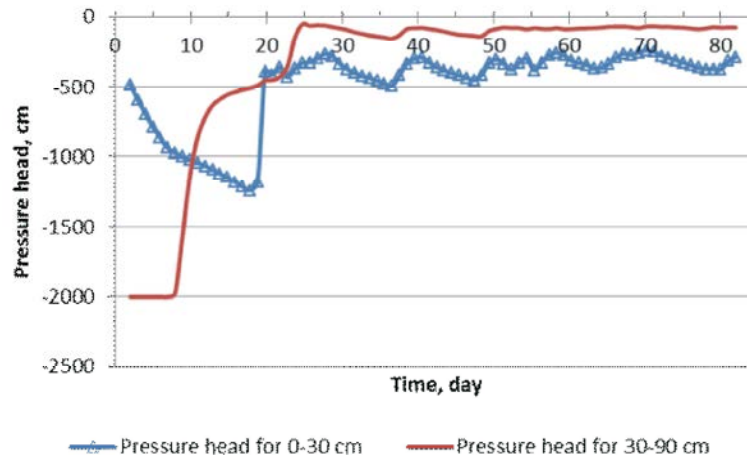


Fig. 2: Measured pressure heads for the 0-30 cm depth and 30-90 cm depth in the soil profile

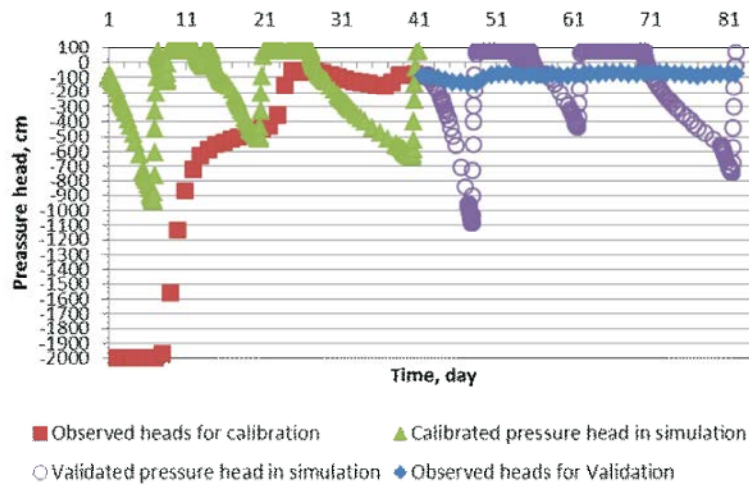


Fig. 3: Observed and simulated pressure head distributions in the soil profile with lateral-1

There were some discrepancies between observed and simulated data and the reasons for these variations may be of multiple sources. However, macropore flow, preferential flow and cracks are considered as the responsible mechanisms [19, 20].

Because the frequency of high intensity rainfall events was very common in the studied rainy period, positive pressure heads developed in all depths in the soil profile. In general, calibration period was less rainy (882.2 cm) than validation period (1292.2 cm). Dry conditions in hot summer caused soil matric potential to reach at -2000 cm at the 30 to 90 cm depth. However, 55% of the observed pressure heads was lower than -100 cm at the 30 to 90 cm layer in the profile during the study. Only 9 pressure head values (11% of the data) were between -1000 and -2000 cm during the 82 days of the study. 58% of the pressure head values during calibration period were below -500 cm (still very wet conditions).

During the validation period, 85% of the pressure heads was between -50 and -100 cm and 100% of the pressure heads were between -50 cm and -200 cm. The extreme pressure head values above -1100 cm (-110 kPa) in the field were because of deep cracks, root and earthworm burrows. In the field, however, equilibrium of the buried moisture probes took at least a day when saturated soil conditions occurred. During the study period, soil profile has shown some positive pressure head values and moisture probes recorded those values to have been 27.4 and 43.7 cm. These wet conditions were also monitored by piezometric head measurements in the study field.

Soil water pressure head gradients displayed very similar pattern of distribution to the observed pressure head values in the soil profile where lateral-1 was buried (Fig. 4). The number of hydraulic gradient peaks and their sequence were very closely matched with each other in the calibration and validation periods of the data.

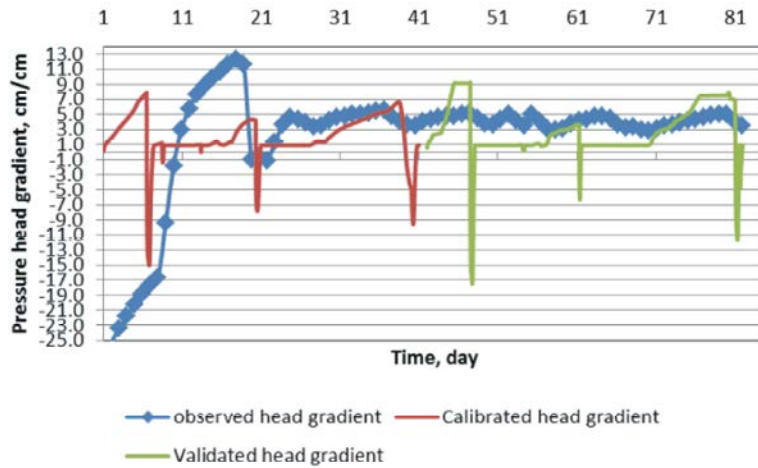


Fig. 4: Observed and simulated pressure head gradients

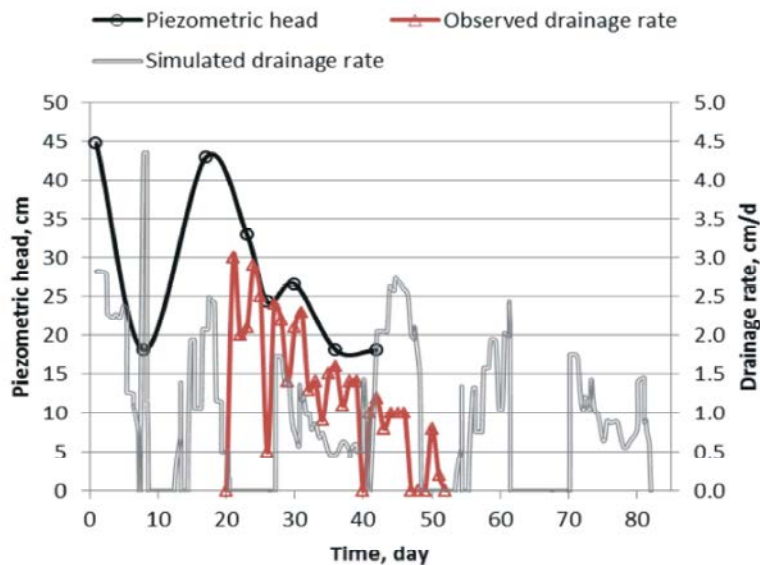


Fig. 5: Observed piezometric heads, drainage rates and simulated tile flows

Where gradients were negative, soil water moved upward direction in the soil profile. Otherwise, water fluxes were always downward direction. There are very steep hydraulic head gradient changes in the soil profile, in which tile pipes were buried. Observed data showed that most of the gradient changes were positive direction oriented. Gradient change ranged between 0.2 and 13 cm/cm in the positive direction, while the range was between 0 and 25 cm/cm in the negative direction.

The piezometers were buried to 120 cm depth that was 30 cm deeper than drain depth in the lateral 1 area. The base of piezometer bore was considered as the arbitrary reference point above the sea level and the corrections of water table level above the tiles were performed by subtracting drain tile elevations from the

piezometer base elevations. Soil piezometric heads ranged between 45 and 17 cm above the lateral 1 during the first study (42 days) (Fig. 5). However, from the day 42 to 82 the field was under flood and no piezometric head and drain flow measurements were recorded. During this period, field hydraulic structures, such as man holes (sumps), the outlets, gages and weirs were not reachable. A total of 1292.2 cm precipitation for the validation period occurred in the field during second half of the study and the second cycle cropping was not carried out in the study area, but also in the region. The observed piezometric heads showed steep fluctuations with 9 day intervals. The fluctuation peaks and dips for piezometric heads were observed to have weekly cycles in the soil profile with lateral-1.

Tile flow rates occurred after piezometric heads reached at 43 cm above the lateral-1 in the soil profile. The fluctuations in the observed drainage rates were much more oscillatory than the one in the piezometric heads in the field. On the day 15, the piezometric head reached at 43 cm height in the profile, drain water started mounting to the tiles. When the piezometric heads started receding, tile flows responded to these recession rates as long as the recession continued. While the piezometric heads declined to 17 cm, drain rates continued to fluctuate on the days between 41 and 52, indicating another groundwater fluctuation pulse arrived at the tiles. The calibration data of tile flows for lateral-1 showed a moderately good agreement with the observed tile flows ($r^2 = 0.246$, $rmse = 0.242$) and the validation of the tile flow rates showed a similar agreement with $r^2 = 0.361$ and $rmse = 0.243$. Cumulative tile flow from the lateral-1 was $-57 \text{ m}^3/\text{ha}$ in the calibration period, while cumulative tile flow in the validation period for lateral 1 was $-84 \text{ m}^3/\text{ha}$. The minus sign showed a net outflow from the lateral pipes to the field outlet.

Simulated tile flows were in moderately good agreement with the observed drain rates during the measurement period. Simulations were carried out for all tile flows during the study period, while the observed drainage rates covered a small period of measurements in the field. The observed and simulated drain rates were high when the piezometric heads were high in the field. The field received no rainfall between the days 42 and 51, as a result of which drain rates decreased sharply. These nine-day simulations showed higher drainage rates than the observed ones. This result may be because saturated hydraulic conductivity used in the hydraulic models was very sensitive to soil matric potentials when soil was drying. Ebrahimian *et al.* [4] found smaller drain rates when the Hooghoudt equation (eq. 6) was used comparing to Hydrus-1D rates. They also reported greater head values as their drain spacing grew larger.

Pressure Head Distribution, Gradients and Simulations for the Latral-3: The pressure head measurements at the 30 to 90 cm depth in the Lateral-3 buried profile of the soil were in wet range of soil water (0 to 100 kPa) (Fig. 6). In contrast to the lateral-1, lateral-3 was in wet conditions and flowing between the days 1 and 20. On the other hand, Lateral-1 was in desiccated conditions during the first 20 days of the study and no tile flow was evident. The oscillatory behaviors of pressure heads in the lateral-3 area were smoother than the one in the lateral-1 area. This meant that saturated conditions around the lateral-3 were

more consistent and long-lived than the ones in the lateral-1 soil profile. The pressure head values ranged from -65 cm to -1112 cm around the lateral-3 in the profile. Two dry periods in the soil were recorded. The first one was between the days 1 and 20 and the other was between the days 37 and 51 (Fig. 1). However, the effect of drought on the lateral-3 buried profile was not as clear desiccation as the one for the lateral-1 buried profile, in terms of pressure head measurements. The soil profile for lateral-3 was predominantly sandy loam and more homogeneous than the lateral-1 buried profile (Table 1). During the simulations, calibration period produced more negative pressure heads than validation period. This could be attributed to the conditions that the calibration period received less rainfall (882.2 cm) than the validation period with 1292.2 cm rainfall. Further, calibration period produced extremely low matric potentials (-6800 cm) specifically in the dry periods of observed values between days 8 thru 19 and days 27 thru 38. Similar trends of pressure head differences occurred in validation period to calibration period. The validation period was more in concert with the observed values for pressure heads. Both calibration and validation periods of the pressure head data produced positive pressure heads between 43 and 47 cm in the lateral-3 buried soil profile. This behavior of lateral-3 was exactly the same as the lateral-1 when the saturated conditions occurred in the soil (Fig. 5 and Fig. 3).

Soil conditions were dominantly wet and the pressure head gradients were mostly around zero for most of the study time (Fig. 6). The negative gradients indicated groundwater recharge and eventually groundwater table was elevated. Positive gradients were more prominent than the negative ones, indicating water flow was from surface to the bottom of the soil. Positive gradients are mostly due to root water uptake in the soil and evaporation from naked surfaces (atmospheric demands). Positive gradients were very common in the calibration period in comparison to validation period in the field. The validation period was dominated by zero gradients of pressure heads, meaning water was inundated on the surface and severe consecutive runoff events occurred in the second half of the study period (days 46-74). On the other hand, the calibration period was dominated by groundwater fluctuations yielding into 4 runoff events (for days between 21 and 28) and drying. Both calibration and validation periods showed good agreements with the observed pressure head gradients (Fig. 7). After the day 22 almost all gradients of observed pressure heads were positive or zero, indicating that frequencies of water table elevation were increased.

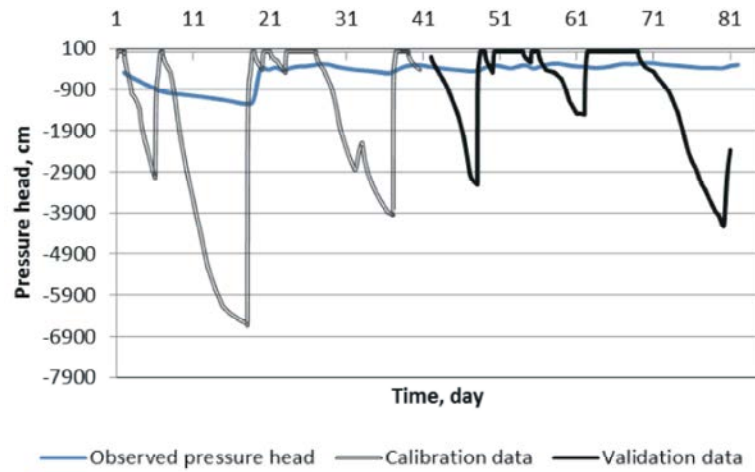


Fig. 6: Observed and simulated pressure heads for the lateral-3 profile of the soil

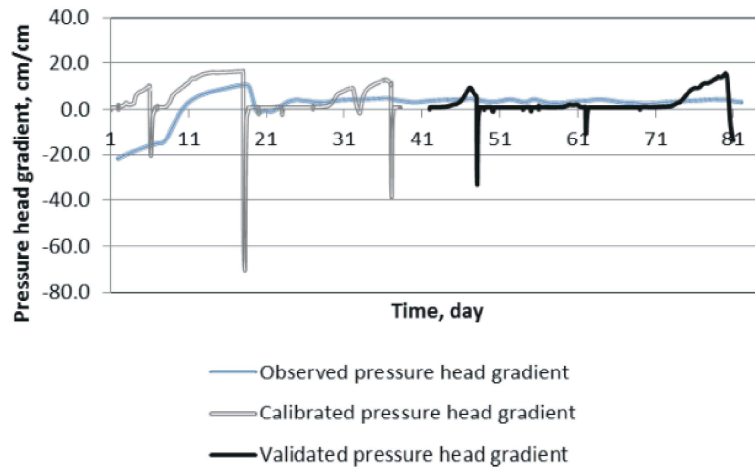


Fig. 7: Observed and simulated head gradients for the lateral-3 profile of the soil

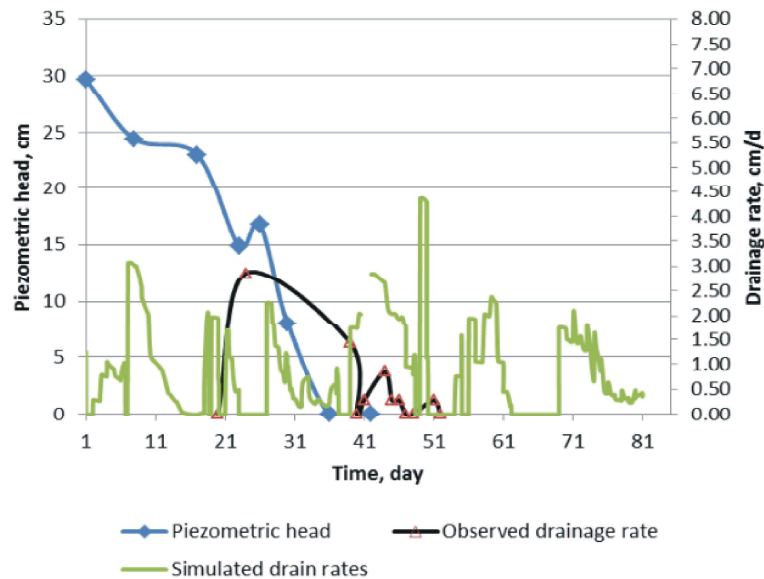


Fig. 8: Observed piezometric heads, drainage rates and simulated tile flows for the lateral-3

Fig. 8 shows piezometric head measurements, observed tile flow rates and simulated tile flows from the lateral-3. The piezometers were buried to 125 cm depth of the soil profile, meaning 125 cm out of the 185 cm piezometer pipe was underneath the soil surface and drain depth versus piezometer base elevations were corrected before piezometric heads were recorded. Therefore, the piezometric head levels were the net piezometric heads above the drainline (lateral-3) in the field. Because of the dry weather conditions and no-rainy period of the first 10-day of the study, piezometer heads dropped from 30 cm to 24 cm. Approximately 8-9 days of rains reached at the groundwater table 10 days after they started (Fig. 1) and this fed groundwater for 10 days, the result of which kept the piezometric head at 24 cm above the tile line by 8 days (Fig. 8). The piezometer head steeply dropped from 23 to 15 cm in 5 days between days 21 and 26. This head drop was compensated partly by a 3-day rainfall occurring in days 19-21, carrying the head to 17 cm height above the tile line in the profile. The piezometric heads continually declined to zero between the days 27 and 36. The head drop in lateral-3 buried profile was much faster than the one in lateral-1 buried soil profile. This may mean that groundwater fluctuation and water table elevations were more frequent than the ones in the lateral-3 buried profile. Besides, lateral-1 area was stayed under high water table conditions than lateral-3 area. This situation was a result of higher saturated hydraulic conductivity in the lateral-3 area than the lateral-1 area, where texture was fine and finer materials in comparison to the lateral-3 area where sandy loam was dominant textural separates in the profile. On the other hand, the lateral-3 area lost more water via outflow discharges than lateral-1 area. It is also evident that steep decline in the piezometric heads in the lateral-3 area is a result of more vertical water flow than lateral flow in the profile upon comparing to the lateral-1 area. Drainage rates from the lateral-3 resembles to the one from lateral-1. However, drainage hydrograph peaks and number of peaks differed from the ones for the lateral-1 hydrograph. Once again, observed drainage rates for lateral-3 were well agreed with the simulated drainage rates from the tiles as was the case for the lateral-1. The base of the drainage hydrograph for lateral-3 was 20 days long, whereas the hydrograph from lateral-1 had a base of 33 days of length.

Simulation and calibration periods of the drain rates for lateral-3 were very similar to the ones for lateral-1. The calibration period of the drainage rates from lateral 3 showed moderately good agreement with the observed

rates in the field ($r^2 = 0.321$, $rmse = 0.423$). On the other hand, the validation period of the drainage rates showed almost the same level of agreement as the data in calibration period with the observed drainage rates ($r^2 = 0.34$, $rmse = 0.833$). Cumulative drain fluxes from the lateral-3 for the calibration period were recorded as (-) 58 m^3/ha , while the validation period yielded in 86 m^3/ha in the field. In the validation period, drain tiles were under the effects of elevating groundwater table. As a result, 86 m^3/ha amount of groundwater entered the lateral-3 in the soil profile (positive sign). This was the major difference between the lateral-1 and the lateral-3. Bouman *et al.* [21] reported 1-2 cm/d water losses in permeable soils profiles and rising runoff depths on the surface could increase these amount.

Simulations were performed for the time interval of 0 to 77 days. The results showed that tile drains acted as zero pressure head potential surface in the soil profile so that all pressure head values around the tiles were between 0 and 96 cm. observed pressure head values were always higher than bottom pressure head values and were higher than simulated ones for the topsoil in the time interval of 0 to 19 days in the study.

Drain Depth and Spacing: Drainage geometry showed that drain spacing and depth in the research field were 37 and 1 m, respectively (from GPS readings in the field). The design parameters for drainage system layout in the field were considered to gradually decline groundwater table in the profile so that any cropping systems in the field could consume the water during hot summer days. As a result, lateral flow discharges are slow and long enough that excess water mounted on the tiles 1-2 days after the piezometric heads elevated. In other words, there were an coincidental head increases in both piezometers and laterals in the soil profile. Drain depth and spacing parameters were not design to remove surface runoff effectively. Drain depth and spacing have an important relationship with each other, which governs the amount of drain discharges to be evacuated from the profile under the main effect of drain spacing rather than drain depth in the soil. In other words, the closer the lateral tiles to each other are, the larger the volume of drainage discharges occurs. In this study, the tile drains removed very small portion of total rainfall. However, discharges could have been increased if the drain spacing could have been small enough to combat surface runoff in the field. Cumulative drain discharges for simulation and observed periods were also under the critical effect of drain depth and

spacing, as well as soil texture. Although cumulative drain discharges were fairly good (barely 8.5 and 12 cm for lateral-1 and lateral-3 for 32 days), silty clay loam (lateral-1) retarded drainage rates more than sandy loam soil (lateral-3).

Drain Rates and Hydrographs: Drain discharge rates sharply increased and decreased based on the piezometric heads above the tile drains. These changes in the discharges occurred almost in daily manner. A consistently low drain rates were observed when the piezometric head was about 17 cm for the lateral-1 and 5 cm for the lateral-3. As the hydrograph base increased, drain rates receded to zero flow value. When the piezometric heads reached 43 and 13 cm, drain rates reached their peak flow rates of 2.9 and 3.1 cm/d between day 20 and 21, respectively for lateral-1 and lateral-3. Drain discharge rates from the lateral-1 was similar to the ones from the lateral-3. However, their hydrographs were different in their peak flows and base lengths, indicating differential amount of total discharges from each lateral in the field. Subsurface drainage system decreased peak flow rates in the silty clay loam soil profile. Drain rates always decreased when the piezometric head ceased to 17 cm above the lateral-1. Drain rates were delayed by low soil hydraulic conductivity and soil texture in the drain depth of the soil profile. For instance, drain rates frequently visited zero values and steep increases based on the water flow to the tile line. A total of 71 m³/ha was recorded by the gage on the lateral-1. This amount of discharge was moderately well agreed with the Hydrus-1D calculated simulations 57 m³ for calibration and 85 m³/ha for validation periods.

For the lateral-3, drainage hydrograph showed that piezometric heads dropped to zero cm, which is equal to drain depth of 90 cm in the profile, drain rates by gravity continued occurring in the profile. As the piezometric heads increased above the tile line, drain discharges increased steeply yielding the highest and largest peak in the flow period of days 20-40. In general, piezometric head of 5 cm corresponded to gravimetric water drainage rates that continued for 11 days after the piezometric head ceased to zero in the profile. Piezometric heads greater than 10 cm resulted in steep drainage rates from the tile line, whereas the rates did not grow larger even if the piezometric heads were greater than 10 cm. This may mean great amount of convergence losses around the tiles occurred and resisted against larger rates of water fluxes to enter the lateral-3. Subsurface drainage system

increased peak flow rates in the sandy loam soil profile. Drainage hydrograph of the lateral-3 showed that the observed drainage rates yielded in 88 m³/ha during the measurement period in the field. This rate of flow is very close to the validation discharges of the drain tile in the profile.

Total discharge volume of the field drains were much higher (264 m³) than the recorded values from lateral-1 and lateral-3. This was because the field had 4 laterals in the soil profile and lateral-2 and lateral-4 were not functioning properly, mostly because they were clogged by fine materials and technical disabilities of recording gages were common especially after high flows accumulating in their sumps, congesting the gage outflows. For calibration and validation periods, the observed drain rates corresponded to 0.23% and 0.284% total runoff (566 cm) for lateral-1 and lateral-3, respectively. On the other hand, the main outlet discharged 0.87% of total runoff volume in this period. This means that surface runoff (31000 m³ of 32 days) can be modified by tile drainage systems. Tile flow discharges were observed before surface runoff flows in the field. This indicated that groundwater table fluctuated before surface runoff started in the field. Big part of stream discharge was due to the tile flows between the days 20 and 25.

CONCLUSIONS

The Amik Plain, Turkey, is vulnerable to heavy Storm water floods and water inundation problems for long years. Agricultural crop production systems and civil infrastructures need surface runoff and groundwater table management (especially drainage water management) measures in the Plain. This study evaluated tile flow effects on soil moisture distribution profile through simulation models to better understand water flow dynamics to tile lines in the soil profile and measured drain rates, piezometric heads and soil water potentials were evaluated against simulation model outputs of tile drainage flow rates under certain initial and boundary conditions. The results of water flow models (hydraulic models) increased our knowledge about water flow in the vadose zone and to the tile lines in the soil profile. Soil unsaturated hydraulic conductivity reached at zero when the negative pressure head (matric head) increased from 0 to -650 cm in the profile. This retarded water transport from the surface of the soil to tile drain lines. The hydraulic flow models also showed that there were number of times groundwater fluctuated and large amount

of groundwater entered the tile lines while the groundwater elevated in the soil profile, which contributed largely to surface runoff and flood damage. Although the hydraulic models were moderately good enough to compare simulation results and observed data, Hydrus-1D still very close drainage flux rates to the observed values, which is considered a very promising outcome to involve the Hydrus-1D in the flood control and management planning strategies. The model simulations showed that soil profile was mostly under wet conditions (pressure head < -500 cm for 53% of the measurement period) as was evident with the observed pressure head values. Tile drainage flow rates depended on drainage geometry (drain depth and space). Soil texture, soil saturated hydraulic conductivity and drain depth and spacing were effective on the tile flows in the profile. The gages on the tiles in the sandy loam site, silty clay loam site and main's outlet showed 88, 71 and 264 m³/ha tile drainage flow discharges during the 32-day measurement period. The main's outlet showed the actively working tile pipes evacuated almost 1% of surface devastating floods, which is a very good indication that surface runoff volumes and their catastrophic effects can be manipulated before they turn into regional disasters. Drainage hydrograph measurements also showed different peak flow rates and durations for lateral-1 (2.9 cm/d, 33 days) and for lateral-3 (3.2 cm/d, 28 days), respectively. This can improve our knowledge to better drainage system design to combat against surface runoff events, sound agricultural water management practices and soil drainage needs in the plain. The groundwater accretion was more effective than surface runoff events to pose a limitation to cropping system in the Amik Plain during the research period. HYDRUS-1D simulations showed that water table elevations ranged from 41 cm to 44 cm for both calibration and validation periods soil profile during 82 days of study. In conclusion, tile drainage systems in the study site have a potential to meet soil drainage needs if they are coupled with watershed level hydrologic models to control and protect flood damage in the field.

ACKNOWLEDGMENTS

This study was supported by Mustafa Kemal University's Science Foundation Directorate (BAP) grants to the project no:1002MKU32.

Conflicts of Interest: The authors declare no conflict of interest.

REFERENCES

1. Korkmaz, H., 2005. Amik Gölü'nün kurutulmasının yöre iklimine etkileri. T.C. Mustafa Kemal Üniversitesi Bilimsel Araştırma Projeleri Fonu. Araştırma Projesi Sonuç Raporu. Proje No: 03 F 0701ç Antakya/Hatay. (In Turkish)
2. Kılıç, Ş., N. Ağca, S. Karanlık, S. Şenol, M. Aydın, M. Yalçın, İ. Özelik, F. Evrendilek, V. Uygur, K. Doğan, S. Aslan and M.A. Çullu, 2008. Amik Ovası'nın detaylı toprak etütleri, verimlilik çalışması ve arazi kullanım planlaması. Mustafa Kemal Üniversitesi Ziraat Fakültesi Toprak Bölümü. Bilimsel Araştırma Projeleri Komisyonu, Proje No: DPT2002K120480. (In Turkish)
3. Phogat, V., A.K. Yadav, R.S. Malik, S. Kumar and J. Cox, 2010. Simulation of salt and water movement and estimation of water productivity of rice crop irrigated with saline water. *Paddy Water Environ.*, 8(4): 333-346.
4. Ebrahimian, H. and H. Noory, Modeling paddy field subsurface drainage using HYDRUS-2D. *Paddy Water Environ.* DOI 10.1007/s10333-014-0465-8.
5. Jolly, I.D., K.L. McEwan and K.L. Holland, 2008. A review of groundwater-surface water interactions in arid/semi-arid wetlands and the consequences of salinity for wetland ecology. *Ecohydrology*, 1: 43-58.
6. Ayars, J.E., P. Shouse and S.M. Lesch, 2009. In situ use of groundwater by alfalfa. *Agric. Water Manag.*, 96: 1579-1586.
7. Šimunek, J., M.T. Van Genuchten and M. Sejna, 2005. The hydrus-1d software package for simulating the one-dimensional movement of water, heat and multiple solutes in variably-saturated media. *Univ. Calif. Riverside Res. Rep.*, 3: 1-240.
8. Crevoisier, D., Z. Popova, J.C. Mailhol and P. Ruelle, 2008. Assessment and simulation of water and nitrogen transfer under furrow irrigation. *Agric Water Manag.*, 95(4): 354-366.
9. Boivin, A., J. Simunek, M. Schiavon and M.T. Van Genuchten, 2006. Comparison of pesticide transport processes in three tile-drained field soils using HYDRUS-2D. *Vadose Zone J.*, 5(3): 838-849.
10. Dash, C.J., A. Sarangi, D.K. Singh, A.K. Singh and P.P. Adhikary, Prediction of root zone water and nitrogen balance in an irrigated rice field using a simulation model. *Paddy Water Environ.* DOI 10.1007/s10333-014-0439-x

11. Day, P., 1965. Particle fractionation and particle-size analysis. In: *Methods of Soil Analysis, Part 1*, CA. Black (ed), Amer. Soc. of Agron. Inc.: Madison, Wisc., 1965; Number 9 Agronomy Series.
12. Klute, A. and C. Dirksen, 1986, Hydraulic conductivity and diffusivity: Laboratory methods. In *Methods of Soil Analysis: Part 1-Physical and Mineralogical Methods*; American Society of Agronomy: Madison, WI, USA, pp: 687-734.
13. Van Genuchten, M.T., 1980. A closed-form equation for predicting the hydraulic conductivity of unsaturated soils. *Soil Sci. Soc. Am. J.*, 44: 892-898.
14. Mualem, Y., 1976. A new model for predicting the hydraulic conductivity of unsaturated porous media. *Water Resour. Res.*, 12: 513-522.
15. Hooghoudt, S.B., 1940. General consideration of the problem of field drainage by parallel drains, ditches, watercourses and channels. Publication No.7 in the series contribution to the knowledge of some physical parameters of the soil. Bodemkundig Instituut, Groningen.
16. Murashima, K. and Y. Ogino, 1985. Design of pipe drainage using the modification coefficient (a). *Trans Jpn Soc Irrig Drain Reclam Eng.*, 119: 13-20.
17. Allen, R.G., L.S. Pereira, D. Raes and M. Smith, 1998. *Crop Evapotranspiration-Guidelines for Computing Crop Water Requirements-FAO Irrigation and Drainage Paper 56*; FAO: Rome, Italy, 300, pp: 6541.
18. Li, H., J. Yi, J. Zhang, Y. Zhao, B. Si, R.L. Hill, L. Cui and X. Liu, 2015. Modeling of soil water and salt dynamics and its effects on root water uptake in Heihe arid wetland, Gansu, China. *Water.*, 7: 2382-2401.
19. Garg, K.K., B.S. Das, M. Safeeq and P.B.S. Bhadoria, 2009. Measurement and modeling of soil water regime in a lowland paddy field showing preferential transport. *Agric. Water Manag.*, 96: 1705-1714.
20. Patil, M.D., B.S. Das and P.B.S. Bhadoria, 2011. A simple bund plugging technique for improving water productivity in wetland rice. *Soil Tillage Res.*, 112: 66-75.
21. Bouman, B.A.M., M.C.S. Wopereis, M.J. Kropff, H.F.M. Berge and T.P. Tuong, 1994. Water use efficiency of flooded rice fields II. Percolation and seepage losses. *Agric Water Manag.*, 26: 291-304.